Applied Geochemistry 114 (2020) 104522

Contents lists available at ScienceDirect

Applied Geochemistry

journal homepage: http://www.elsevier.com/locate/apgeochem

Hydrogeological controls of arsenic and uranium dissolution into groundwater of the Pine Ridge Reservation, South Dakota

Kenneth Swift Bird [a,*], Alexis Navarre-Sitchler [a,b], Kamini Singha [a,b]

[a] Hydrologic Science & Engineering Program, Colorado School of Mines, Golden, CO, 80401, USA
[b] Department of Geological Engineering, Colorado School of Mines, Golden, CO, 80401, USA

ARTICLE INFO

Handling Editor: Prof. M. Kersten

Keywords:
Arsenic
Uranium
Pine Ridge Reservation
Principal component analysis
Cluster analysis

Abstract: This study integrates geochemical modeling, spatial analysis and several statistical methods including principal component analysis, multivariate regression and cluster analysis to investigate hydrogeologic controls of arsenic and uranium contamination within groundwater of the Arikaree aquifer on the Pine Ridge Reservation (PRR). Located in southwestern South Dakota, the PRR is largely rural and many people rely on domestic supply wells completed in the Arikaree aquifer as their primary drinking water source. Locally, the White River Group, which unconformably underlies the Arikaree Group, is enriched in arsenic and uranium related to volcanic ash deposits and acts as a geogenic metal source. Geochemical data from over 250 groundwater samples were obtained through collaboration with the Oglala Sioux Tribe. Cluster spatial statistics analyses delineated four regions of statistically significant variations in groundwater chemistry that represent upgradient, intermediate, and downgradient portions of the Arikaree aquifer. Groundwater evolves as it flows through the Arikaree aquifer with increasing alkalinity, sodium, and pH along flow paths. These chemical changes are likely due to dissolution of carbonate minerals and volcanic ash. Thermodynamic calculations suggest increasing supersaturation of the groundwater with respect to calcite; thus, volcanic ash dissolution may be an important secondary source of alkalinity. Elevated alkalinity and pH levels were found to be the driving factors of arsenic and uranium mobility, and downgradient sections of the aquifer in the northern portions of the PRR are most likely to be impacted by metal(loid) contamination, with 73% of the wells in this grouping failing a USEPA maximum contaminant level for arsenic, uranium, and/or gross alpha.

Abstract

1. Introduction

Native American tribal populations are known to face greater health concerns compared to other population groups in the U.S. (Jones, 2006). Part of this disparity is access to water; community water systems often underserve tribal populations, as many reservations are located in rural parts of the country with a dispersed population base. 8.9% of tribal homes lack access to safe drinking water, compared to 0.6% of non-Native American homes (IHS, 2008). Additionally, contamination is an issue; most tribal lands are located in the western United States, which coincides with the majority of U.S. heavy-metal mineral deposits; up to 75% of uranium mines in the U.S. are within 50 miles of a Native American Reservation (Shacklette and Boerngen, 1984; Blake et al., 2017; Lewis et al., 2017).

Heavy metal mineralization is often dispersed over tens to hundreds of kilometers resulting in non-point sources capable of affecting regional water quality (e.g., Colman, 2011; Focazio et al., 1999). Heavy-metal contamination in groundwater is typically attributed to anthropogenic activities such as mining operations and the subsequent industrial use of metals. However, groundwater contamination can also occur by natural mineral dissolution, leaching, and transport in areas with localized high concentrations of arsenic (As) or uranium (U) in bedrock and/or soils (Braithwaite et al., 2008). The U.S. Environmental Protection Agency (USEPA) maximum contaminant levels (MCLs) for As and U are 10 μg/L and 30 μg/L, respectively (USEPA, 2000; USEPA, 2001), as these metals can have adverse health effects on the liver, heart, and kidneys, and are carcinogenic (Milvy and Cothern, 1990; Smith et al., 1992). Quantifying controls of contaminant mobilization as well as transport pathways are crucial to assessing risk and developing planning and remediation

* Corresponding author.
E-mail address: kenny.swiftbird@gmail.com (K. Swift Bird).

https://doi.org/10.1016/j.apgeochem.2020.104522
Received 24 April 2019; Received in revised form 30 December 2019; Accepted 2 January 2020
Available online 3 January 2020
0883-2927/© 2020 Published by Elsevier Ltd.

strategies in tribal communities affected by heavy metal exposure.

Here, we explore controls on the mobilization of As and U in groundwater on the Pine Ridge Reservation (PRR) in southwestern South Dakota. The PRR encompasses nearly 9000 km^2 roughly 75 km southeast of the Black Hills, the state's most prominent geological feature (Fig. 1). The PRR is the seventh largest reservation by area in the U.S. and is home to the Oglala Sioux Tribe, which has approximately 19,000 people according to census data from 2010 (U.S. Census Bureau, 2010). The climate of the PRR is semi-arid, and the landscape is marked by rolling fields of prairie grasslands, broken by sandstone buttes in the south and undulating badlands in the north. Most land on the PRR is not suited for farming due to low rainfall and associated droughts, but many of the prairie grasslands are ideal for cattle ranching. Previous studies of water quality on the PRR have found elevated concentrations of As and U up to 77 ppb and 60 ppb, respectively, in groundwater (Heakin, 2000; LaGarry and Yellow Thunder, 2012), and residents of the PRR have a 40% higher cancer mortality rate than the rest of the U.S. population (Rogers and Petereit, 2005). Public health research suggests that tribal residents from the PRR are more likely to be exposed to As, U, and tungsten (W) than any other demographic group in the U.S. (Pang et al., 2016). Here, we focus on underlying hydrogeochemical controls of heavy metal dissolution and mobility on the PRR for which little to no published research exists. We apply several geostatistical methods to existing geochemical data, and complete geospatial mapping of those data to assess whether any regions or geologic units are particularly susceptible to contamination impacts from As and U dissolution. These analyses are then synthesized to develop a conceptual model for As and U dissolution on the PRR based on local hydrogeology and geochemistry.

2. Background

2.1. Pine Ridge Reservation geology

The source of As and U in groundwater on the PRR is mineralization from volcanic ash emplaced into the White River Group and Arikaree Group, which span parts of the PRR and the surrounding area (Fig. 2; Table 1) (Carter et al., 1997; Heakin, 2000; Kipp et al., 2009). The Arikaree Group serves as the primary aquifer for domestic wells, and groundwater generally flows from south to north (Fig. 2) (Carter and Heakin, 2007). The potentiometric surface of the Arikaree aquifer is controlled by surface topography and major rivers, as the Arikaree Group dips less than 1° (Rahn and Paul, 1975).

The basal portion of the Arikaree Group is known as the Rockyford Ash Zone and has significant levels of volcanic ash, which are not sufficiently concentrated in U to be considered economic grade but could impact water quality (McConnell and Dibenedetto, 2012). However, the White River group is primarily composed of bentonite (weathered volcanic ash) and does contains ore-grade U mineralization. A major deposit (14 million kg U_3O_8 with a grade in excess of 0.25% U by weight) was discovered in the White River Group near Crawford, Nebraska and this deposit is currently mined via in-situ leaching (Gjelsteen and

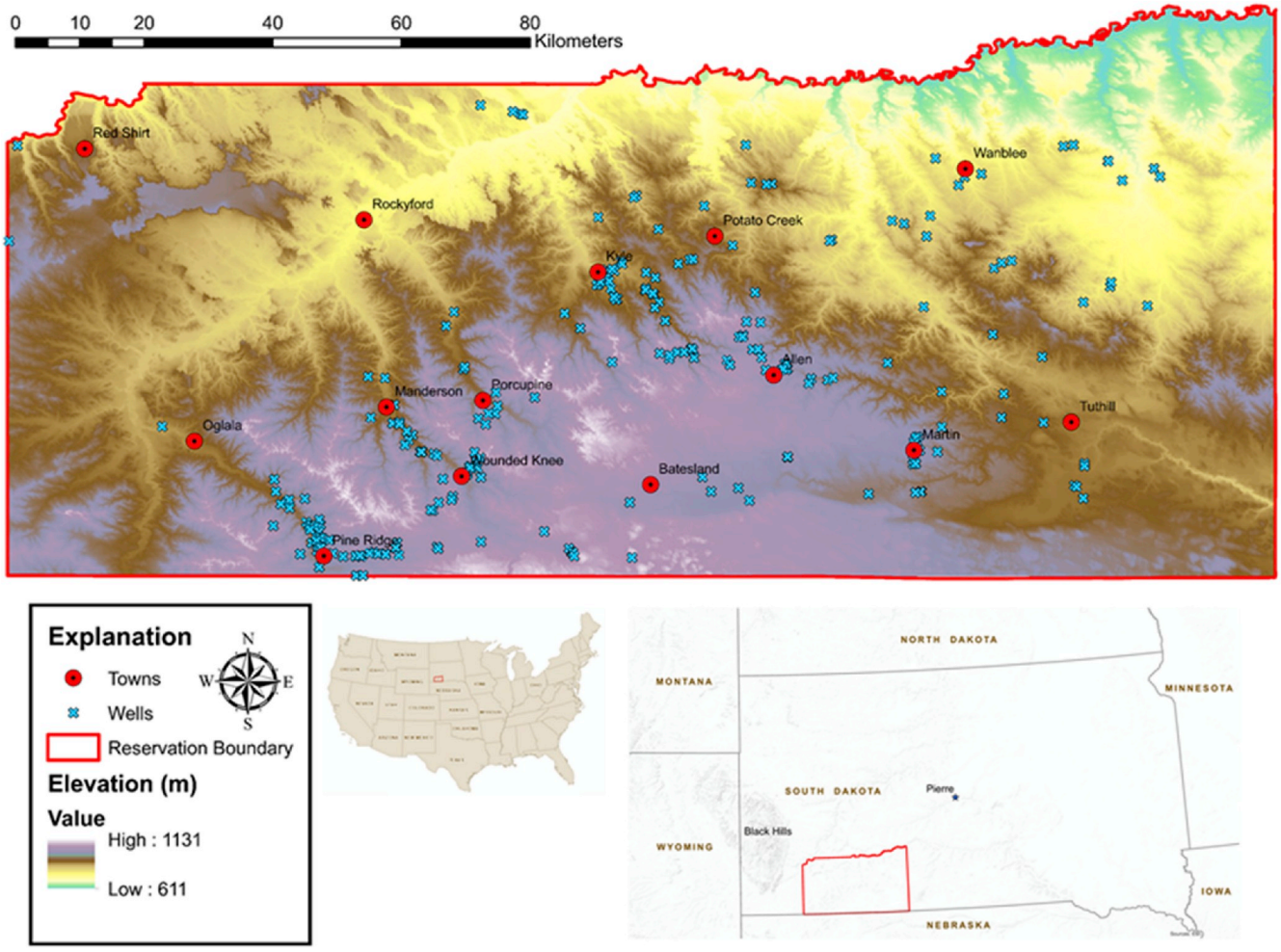

Fig. 1. Map showing the extent of the Pine Ridge Reservation (PRR) in SW South Dakota. Groundwater well locations, surface elevation and town centers are also detailed on the map.

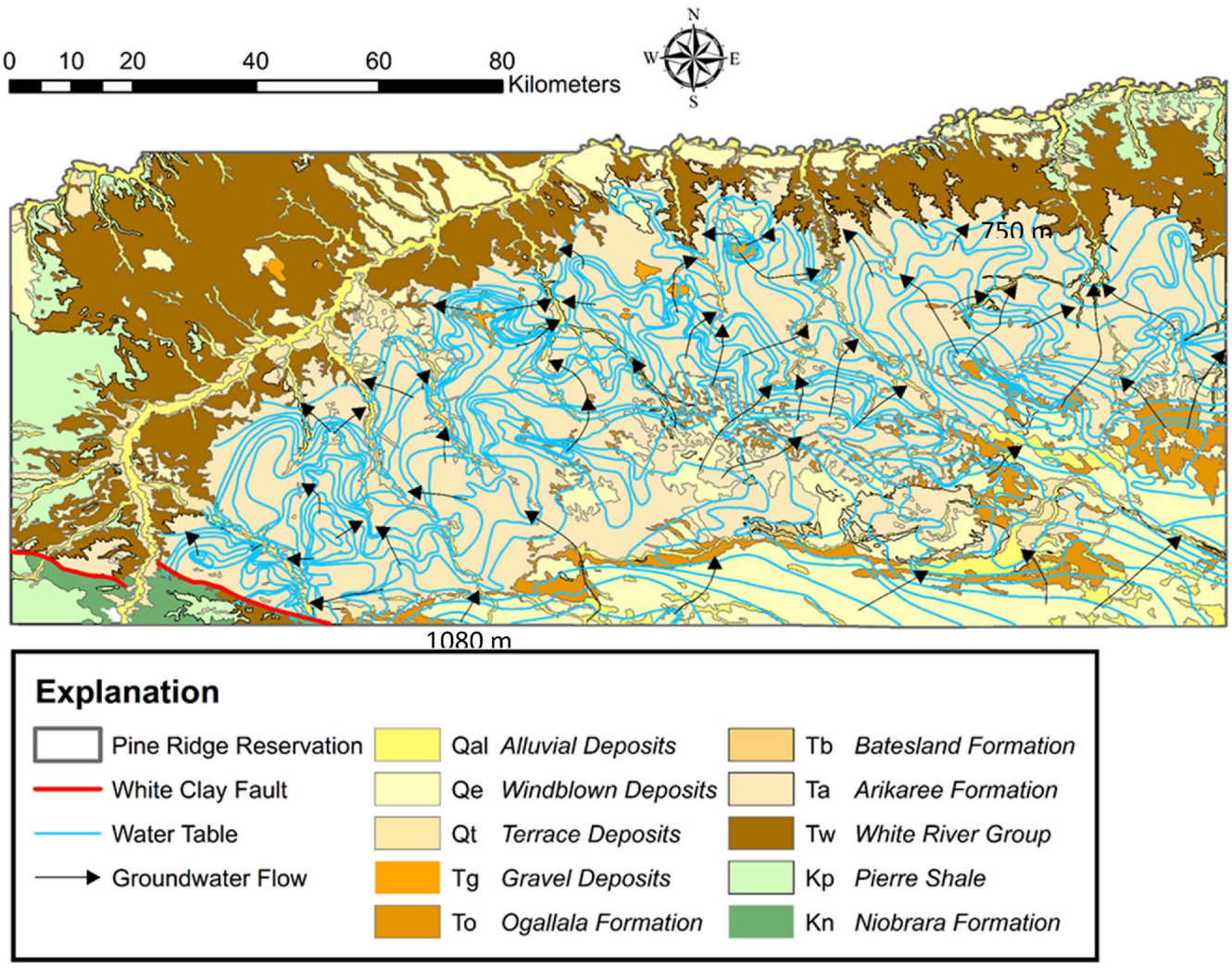

Fig. 2. Map detailing geologic units of the PRR at a 1:500,000 scale (Martin et al., 2004) overlain by generalized groundwater flow lines for the PRR based on potentiometric contours (contour intervals of 15 m) of the Arikaree aquifer (Carter and Heakin, 2007).

Table 1
Stratigraphic column modified from Heakin (2000) detailing geologic formations present on the PRR. Thickness and lithology of the units and subunits (when present) are also noted.

Period	Epoch	Unit	Subunit	Thickness (m)	Lithology
Quaternary	Holocene & Pleistocene	Alluvial, Eolian & Terrace Deposits		0–60	Sand, silty clay & gravel
Tertiary	Pliocene	Ogallala Formation		0–60	Tan, fine to medium grain sandstone
	Miocene	Batesland Formation		0–15	Cross-bedded sand interbedded w/silts, clays & marls
		Arikaree Group	Unit E (Rosebud Form.)	0–72	Tan, calcareous sand, silt & clay
			Unit D (Harrison Form.)	0–38	Fine, gray sand w/marl, several pipey and spherical concretions
			Unit C (Monroe Creek Form.)	0–28	Fine grained sandstone & siltstone
			Unit B (unnamed)	0–115	Pinkish tan, consolidated silt and sand w/limestone lenses and channel sands
			Unit A (Sharps Form.)	0–15	White, tan, & reddish brown volcanic ash interbedded w/silt
	Oligocene	White River Group	Brule Form.	0–140	Yellow to brown, poorly consolidated siltstone & claystone
			Chadron Form.	0–34	Greenish-gray bentonite clay w/alternating layers of siltstone
Cretaceous	Upper Cretaceous	Pierre Shale		0–365	Dark gray marine shale w/bentonite
		Niobrara Formation		0–100	Gray to tan, calcareous shale

Collings, 1988; Hansley et al., 1989). On the PRR, U mineralization is particularly favorable in paleochannels in the White River Group, such as the remnants of the Red River Valley near Red Shirt (Raymond et al., 1976; Dickinson, 1993).

2.2. Arsenic and uranium geochemistry

Arsenic (As) can occur in the environment in several oxidation states, but the most prevalent forms are arsenite (As(III)) and arsenate (As(V)). As(V) is generally more soluble than the more toxic As(III), but also has higher sorption affinity. Both arsenate and arsenite typically exist as oxyanions and are stable over pH ranges typically found in groundwater in both oxidizing and reducing environments (Nordstrom et al., 2014). As mobility in groundwater is often controlled by sorption/desorption reactions with iron (Fe) and manganese (Mn) oxides, which are common components of sands, silts and clays (Bowell, 1994). As(III) and As(V) can occur together in groundwater due to redox disequilibrium (Bowell et al., 2014). As(III) can form complexes with carbonate in anaerobic conditions, and competition between As and carbonate species for sorption sites also occurs, which enhances As mobility (e.g., Holm, 2002; Lee and Nriagu, 2002). As mobility is difficult to generalize in subsurface environments given that it can be mobile over both oxidizing and reducing conditions. However, As(III) and As(V) mobility is generally controlled by sorption processes which can limit mobility of these species, particularly at lower pH levels (e.g. Stollenwerk, 2005).

Uranium (U) has two oxidation states that are stable in natural environments: U(IV) and U(VI). The U(IV) phase exists under reducing conditions, and is generally considered to be immobile, as it forms insoluble minerals such as uraninite (UO_2) (Adler, 1963). U(VI) dominates in oxic conditions, and strongly sorbs to Fe (oxy)hydroxides in the pH range typically found groundwater limiting U(VI) mobility (e.g., Waite et al., 1994). However, U(VI) readily forms several stable aqueous complexes with carbonate, limiting U(VI) sorption affinity and keeping it mobile in groundwater systems (e.g., Cumberland et al., 2016; Singh, 2010). Additionally, nitrate (NO_3^-) can mobilize U by oxidizing U(IV) to U(VI), particularly in shallow wells where infiltration rates exceed microbial reduction rates (Nolan and Weber, 2015). Reactions with NO_3^- are especially prevalent in agricultural areas due to farming and ranching runoff. Together, redox chemistry, alkalinity, adsorption, complexation and NO_3^- levels typically co-control the fate and transport of U in subsurface environments (eg. Beaucaire and Toulhoat, 1987; van Berk and Fu, 2017; Zachara et al., 2013).

3. Methods

Geochemical data and wells logs were compiled from a sampling campaign conducted by the Indian Health Service (IHS) on the PRR. Part of IHS's mission is to provide clean and safe water and sanitation infrastructure to tribal lands, which involves constructing domestic drinking water wells in remote locations. IHS installed 253 domestic wells on the PRR between 1990 and 2016. Once well construction was completed, IHS then sampled wells for water quality including measurements of gross alpha, As, U, pH, and major inorganic parameters such alkalinity, nitrate (NO_3^-), sulfate (SO_4^{+2}), sodium (Na^+), potassium (K^+), magnesium (Mg^{+2}), iron (Fe), chloride (Cl^-), fluoride (F^-), manganese (Mn^{2+}), and barium (Ba^{+2}). Geological strata, well screen depth, and total borehole depth were collected from well logs where available (~75% of wells). Water testing was completed at professional facilities using established USEPA protocol, either the State Public Health Lab in Pierre, SD or at Energy Laboratories in Rapid City, SD. IHS then compared sampling results to USEPA MCL standards, even though MCL standards are not enforceable in private wells (U.S. EPA, 1991a). A point-of-use filter was applied to any well water that did not meet MCL standards for As, U, or gross alpha.

These water quality reports, well logs (when available), and well GPS locations were obtained through collaboration with the Oglala Sioux Tribe and the Martin field office of the IHS and compiled into a database. Direct measurements of aqueous U concentration were only completed in ~40% of the total wells (107 wells); instead, gross alpha, which measures total radioactive decay by alpha emission, was used as a proxy for radionuclide concentration in water. A common assumption is that 2/3 of gross alpha emission (pCi/L) is the result of U concentration in water (μg/L) (USEPA, 2015). To estimate U concentrations in groundwater when only gross alpha levels were measured, a 2/3 scaling approach and a linear correlation between U and gross alpha were compared against one another. We found simple 2/3 scaling and a linear correlation between gross alpha and U were nearly identical in terms of fit (both had a Pearson's $r^2 \sim 0.6$). However, scaling gross alpha by 2/3 predicted lower U concentrations and was the more conservative approach. Thus, when U concentration was not measured by IHS, we estimated U levels by scaling gross alpha concentrations by 2/3. If any geochemical parameters were below analytical detection limits, the concentration was assumed to be one half of the detection limit for statistical analyses (U.S. EPA, 1991b).

Once data compilation was complete, the data were analyzed for potentially distinct geochemical environments, groundwater provenance, and to assess how differences in groundwater chemistry affect subsurface mobility of As and U. All parameters were log transformed prior to statistical analyses to minimize influences from extreme values. Geochemical measurements are often skewed right, but commonly display log-normal distributions (Helsel and Hirsch, 2002). MATLAB was used for statistical analysis and several approaches were employed to explore relationships between geochemical variables. Agglomerative clustering was first used to identify potential geochemical environments, and multivariate regression and principal component analysis were then used to parse geochemical parameters that influence As and U mobility on the PRR. Spatial analysis was also completed in ArcGIS to assess whether trends in As and U concentration are related to bedrock geology. Finally, geochemical equilibrium modeling was used to quantify mineral precipitation and dissolution rates in each of the distinct geochemical environments, which can affect mobility of As and U.

3.1. Statistical methods

3.1.1. Agglomerative clustering

Agglomerative clustering was used to group the borehole geochemical data according to their similarity. Clustering can either be completed to identify natural sample groupings (Q-mode), or variable groupings (R-mode); for example, in water quality studies, Q-mode clustering shows groups that may represent similar geochemical environments, and R-mode clustering shows geochemical parameters that may be interrelated (Meng and Maynard, 2001). Here, Q-mode clustering was used to identify possible geochemical environments using the cosine theta similarity coefficient between different well samples. This method is commonly employed in Q-mode clustering, and it operates by converting samples into vectors, and measures the cosine of the angle between vectors as shown below:

$$similarity = \cos(\theta) = \frac{A \cdot B}{||A||||B||} = \frac{\sum_{i=1}^{n} A_i B_i}{\sqrt{\sum_{i=1}^{n} A_i^2}\sqrt{\sum_{i=1}^{n} B_i^2}}. \quad (1)$$

Thus, the cosine theta similarity coefficient is particularly useful in water quality studies as it is only sensitive to proportions between variables rather than absolute magnitudes of the geochemical parameters. This allows water-quality measurements on different scales (i.e. logarithmic pH scale, major ions in mg/L, and trace metals in μg/L) to be analyzed together without biasing results from differences in magnitude.

3.1.2. Multivariate regression

Multivariate regression can be a powerful tool in water-quality studies because it considers all possible interactions between

geochemical parameter combinations to develop a conceptual model for a given response variable (e.g., Davis, 2002). In this case, a suite of geochemical measurements including pH, alkalinity, major ions, and metals were used as indicator variables to predict concentrations (responses) of As and U in each of the distinct geochemical environments. Multivariate regression was completed on log-normalized data to limit the effects of skewness within the water quality data on data analysis (e.g., Hirsch et al., 1991). Log-normalized data also allowed for more uniform weighting of the multivariate regression to indicate which geochemical parameters have the greatest impact on As and U levels. Multivariate regression models have different methods for handling the intercept of the regression. Single intercept models employ only one intercept, similar to bivariate regression, while models with a dynamic intercept have several intercepts for various parameter and interaction groupings. For simplicity, this study used a single-intercept model, which is a more conservative approach to multivariate regression as the intercept remains quasi-linear rather than changing in high-order dimensions. To avoid overfitting, the Akaike Information Criterion (AIC) was calculated to select the "best" model that employed the fewest parameters (e.g., Bozdogan, 1987). Separate models were developed for As and U, as these two metals have different controls on speciation, solubility, and mobility.

3.1.3. Principal component analysis (PCA)

Principal Component Analysis (PCA) is a data compression technique that reduces high-dimension data sets (such as water quality reports) into key components via singular value decomposition (SVD) (e.g., Wold et al., 1987). PCA rotates the original data into a set of new orthogonal variables known as principal components, which are a set of uncorrelated factors ordered so that the first few components describe most of the variation present in the data set (Jolliffe, 2002). PCA analysis can identify any underlying structure of variance within a dataset (e.g., Abdi and Williams, 2010), which is particularly useful to identify key parameters in water-quality studies because many variables, such as pH and alkalinity, are often interrelated. Groundwater samples were not split into groups for this assessment, and U concentrations were omitted from PCA analysis to avoid autocorrelation with gross alpha measurements. Gross alpha was chosen to represent radionuclide concentrations because it was measured in all wellbore samples in the dataset.

3.2. Spatial methods

Geospatial analysis was completed in ArcGIS 10.5. South Dakota bedrock geology was obtained from the South Dakota Geological Survey, and the 10 m Digital Elevation Model data product from the U.S. Geological Survey (USGS) (Archuleta et al., 2017). These maps were produced to show general topography and groundwater flow of the PRR (Fig. 2). Additionally, distinct well groups found via agglomerative clustering were plotted against bedrock geology of the PRR to determine if any of the groupings related to changes in subsurface geological strata.

3.3. Geochemical modeling

Samples from distinct geochemical environments, indicated by agglomerative clustering, were averaged together. These aggregate samples were used for equilibrium modeling in Geochemist's Workbench (GWB) following methodology from Meng and Maynard (2001). Mineral saturation indices were calculated at 25 °C using the thermo.tdat thermodynamic database distributed with GWB to evaluate the potential impact of mineral precipitation and dissolution on As and U mobility.

4. Results

Clustering, multivariate regression, PCA, and geochemical modeling were used to assess factors that influence subsurface mobility of As and U on the PRR. Results for each method are detailed below.

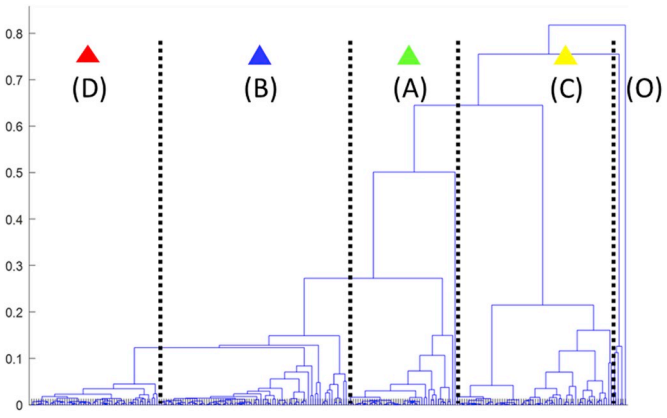

Fig. 3. Dendrogram of Q-mode analysis of PRR water chemistry. There are five distinct clusters that can be seen in this analysis. Each of the four significant groupings was assigned a color, from left to right: red, blue, green, and yellow. This color scheme was used for further analysis that indicated these groupings are clustered both by major ion geochemistry (Fig. 4) and spatially (Fig. 6). (For interpretation of the references to color in this figure legend, the reader is referred to the Web version of this article.)

Table 2
Mean values representing composite geochemistry for each of the four major geochemical clusters and the fifth outlier group.

Cluster Group	Region A	Region B	Region C	Region D	Outlier Group
Well Depth (m)	64.6	63.4	66.4	54.7	23.1
# of Wells	46	80	67	54	6
U (ppb)	5.0	8.5	9.6	13.0	3.3
As (ppb)	6.1	6.9	11.9	11.6	23.0
Gross Alpha (pCi/L)	6.5	10.6	12.7	15.8	4.9
pH	7.8	7.8	8.0	8.1	7.5
Alk (mg/L as $CaCO_3$)	172	202	208	252	215
TDS (mg/L)	270	397	359	374	289.7
NO_3^- (ppm)	1.4	1.2	0.9	0.9	1.5
SO_4^{-2} (mg/L)	20.9	78.1	41.9	34.1	39.4
F^- (mg/L)	0.4	0.4	0.5	0.5	0.6
Cl^- (mg/L)	19.6	9.6	9.0	8.6	5.6
Ca^{+2} (mg/L)	51.9	56.3	36.2	23.5	57.7
Mg^{+2} (mg/L)	7.6	8.8	4.9	2.0	9.1
K^+ (mg/L)	8.6	11.6	10.0	10.3	10.0
Na^+ (mg/L)	18.8	51.8	70.4	101	41.4
Fe (ppb)	36.8	50.2	1660	56.3	30.3
Mn (ppb)	24.4	36.6	60.0	13.3	2090
Ba^{+2} (ppb)	206	93.6	136	46.2	1140

4.1. Cluster & spatial analysis

Agglomerative clustering identified distinct groupings that may represent geochemical environments on the PRR (Fig. 3). There were four major clusters, and a fifth grouping of outliers with only six wells that was not considered further in any statistical or geochemical methods because of the low number of wellbore samples (Table 2). Samples from each of the four significant groupings were plotted in a Piper Diagram (Fig. 4) to delineate major differences in wellbore geochemistry within the dataset. The four geochemical groupings identified by agglomerative clustering parsed into different sectors of the Piper plot, indicating that the clusters represent distinct geochemical environments on the PRR.

Region A wells are generally clustered in the southern, upgradient portions of the aquifer proximal to contacts with overlying formations and had the lowest TDS levels Fig. 5. Region B had the highest levels of

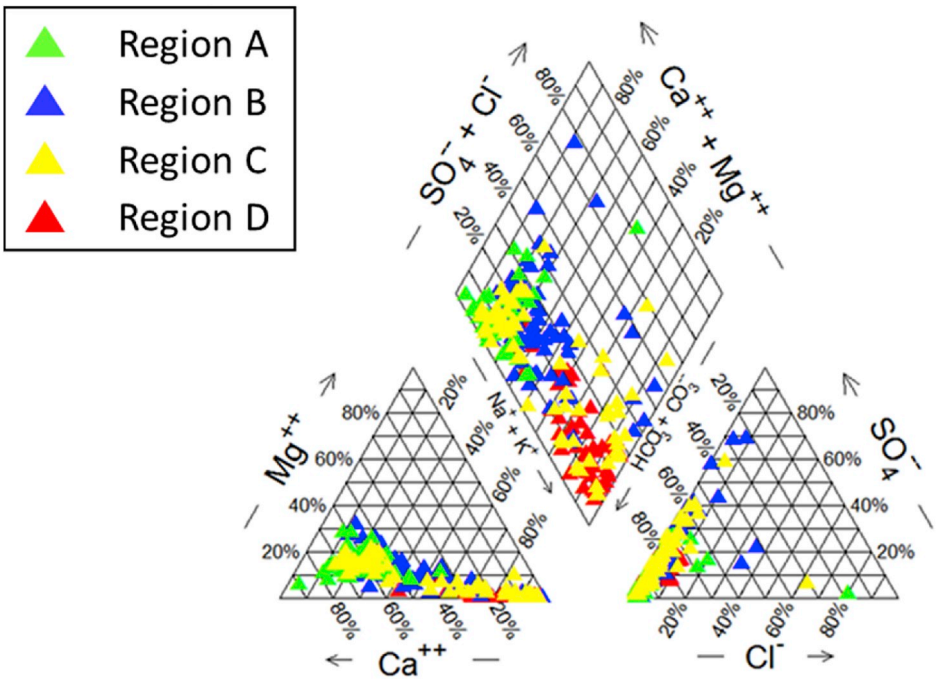

Fig. 4. Piper diagram showing the relative proportions of major ions in PRR groundwater for the four geochemical regions. Waters are generally rich in Na^+ or Ca^{2+} compared to Mg^{2+} and have low relative proportions of Cl^-, with most waters dominated by carbonate species.

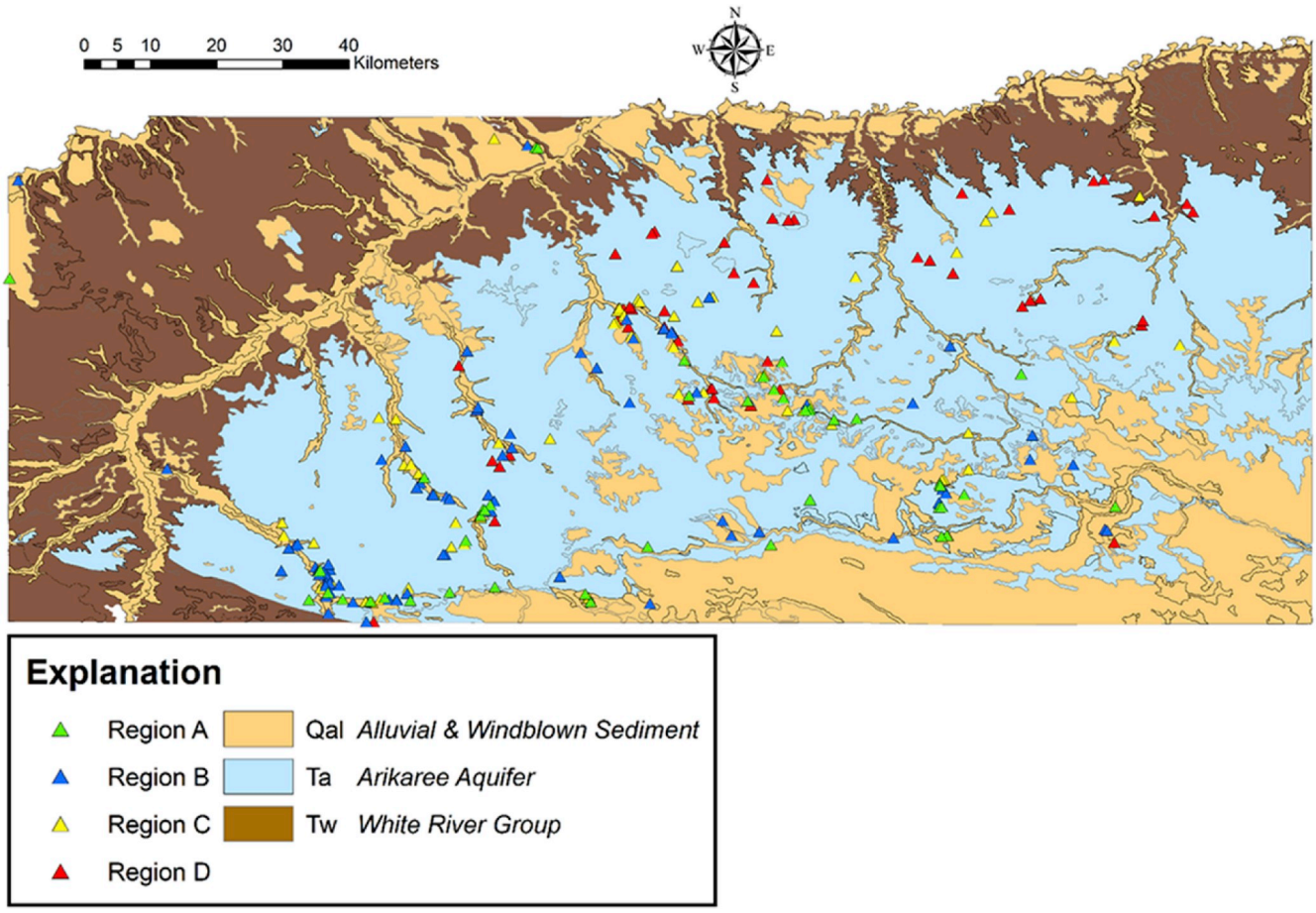

Fig. 5. Spatial plots of Regions A-D showing their relative position within the Arikaree aquifer.

Table 3
Log transformed multivariate regression models for arsenic and uranium concentration in each of the four geochemical groupings.

Grouping:	Arsenic (As) (ppb)	Uranium (U) (ppb)
Region A	As = -7.16 + 9.69*(pH) −0.251*(NO_3^-) – 0.199*(Cl^-) + 0.487*(K^+) −0.574*(Fe) + 0.785*(F^-)	U = −1.04 + 0.960*(Alk) – 0.134*(Fe)
Region B	As = 1.75–0.113*(SO_4^{-2}) - 0.442* (Ca^{+2}) + 0.371*(F^-)	U = −1.92 + 1.18*(Alk) + 0.166*(SO_4^{-2}) −0.145*(Fe) −0.230*(F^-)
Region C	As = 1.53–0.492*(Ca^{+2}) – 0.313* (Fe) + 0.253*(Mn) + 0.450* (Ba^{+2}) + 0.843*(F^-)	U = −0.502 + 0.195*(NO_3^-) + 0.483*(Ca^{+2}) – 0.568*(K^+) + 0.663*(Na^+) + 0.218*(Fe) – 0.249*(Mn)
Region D	As = 4.62–4.16*(pH) - 0.128* (NO_3^-) - 0.292*(SO_4^{-2}) – 0.330* (Na^+) + 0.213*(Mn) + 1.21*(F^-)	U = −9.03 + 7.31*(pH) + 0.576*(Ca^{+2}) −0.623*(K^+) + 0.330*(Na^+) – 0.382*(F^-)

SO_4^{-2}, and is clustered primarily in the south-central portions of the aquifer. Region C had significantly higher Fe levels than any of the other groupings and is located in the central portion of the Arikaree aquifer. Region D is primarily located in the northern, downgradient sections of the Arikaree aquifer and was enriched in Na^+, pH and alkalinity.

4.2. Multivariate regression

Multivariate regression was used to parse geochemical parameters capable of influencing As and U mobility on the PRR in the four major geochemical regions (Table 3). To find the optimal fit, stepwise regression was used to combine geochemical parameters (i.e. pH, alkalinity, major ions, and trace metals) until the "best" model that employed the fewest parameters was found according to the Akaike Information Criterion (AIC). In Region A, As mobility is enhanced primarily by increasing pH, while U mobility positively relates to alkalinity levels. F^- is the strongest multivariate predictor of As levels in Regions B, C, and D and could indicate proximity to volcanic ash deposits, which commonly acts as a geogenic source of both ions (Armienta et al., 2011; Masuda, 2018).

The results of the multivariate regression may show a sensitivity to redox processes. U is more mobile in oxic zones, and was positively correlated with NO_3^- and SO_4^{-2}, which are prevalent in oxic conditions, seen in Regions B and C. As concentrations were negatively correlated with NO_3^- and SO_4^{-2} in Regions B and D, which could indicate its speciation is primarily arsenite As(III), which is the dominant As species in reducing conditions. As was negatively correlated with Fe in regions A, B, and C. Similarly, U was negatively correlated with Fe in regions A and B. While not tested further here, this negative correlation is consistent with general behavior of metal mobility where As and U concentrations in groundwater can be controlled by sorption onto Fe (hydr)oxides where present (e.g. Nagorski and Moore, 1999). However, this negative correlation between U and Fe did not hold in Region C, which had significantly higher Fe levels than any of the other groups (Fig. 6); dissolution of Fe (hydr)oxides in a more reducing environment could release adsorbed As in this region, while multivariate results suggest that uranium levels may be influenced by Mn sorption.

4.3. Principal component analysis

PCA was then completed on the log normalized dataset. This dimension-reduction technique identified four key principal components representing 25%, 21%, 14.8%, and 11.8% of the total variance within the dataset, which cumulatively explain 73% of the variation in groundwater geochemistry. These principal components were then plotted against one another to further delineate geochemical differences between the various regions of the Arikaree aquifer (Fig. 7). The first principal component splits PRR groundwater geochemistry into upgradient portions of the Arikaree aquifer, which are characterized by high Ca^{2+}, Mg^{2+} and to a lesser extent NO_3^- concentrations, and downgradient portions of the aquifer which are enriched in Na^+ and Fe^{2+}. The third and fourth principal components are controlled by NO_3^-, SO_4^{2-}, and Fe^{2+}, which may be indicative of redox processes within the Arikaree

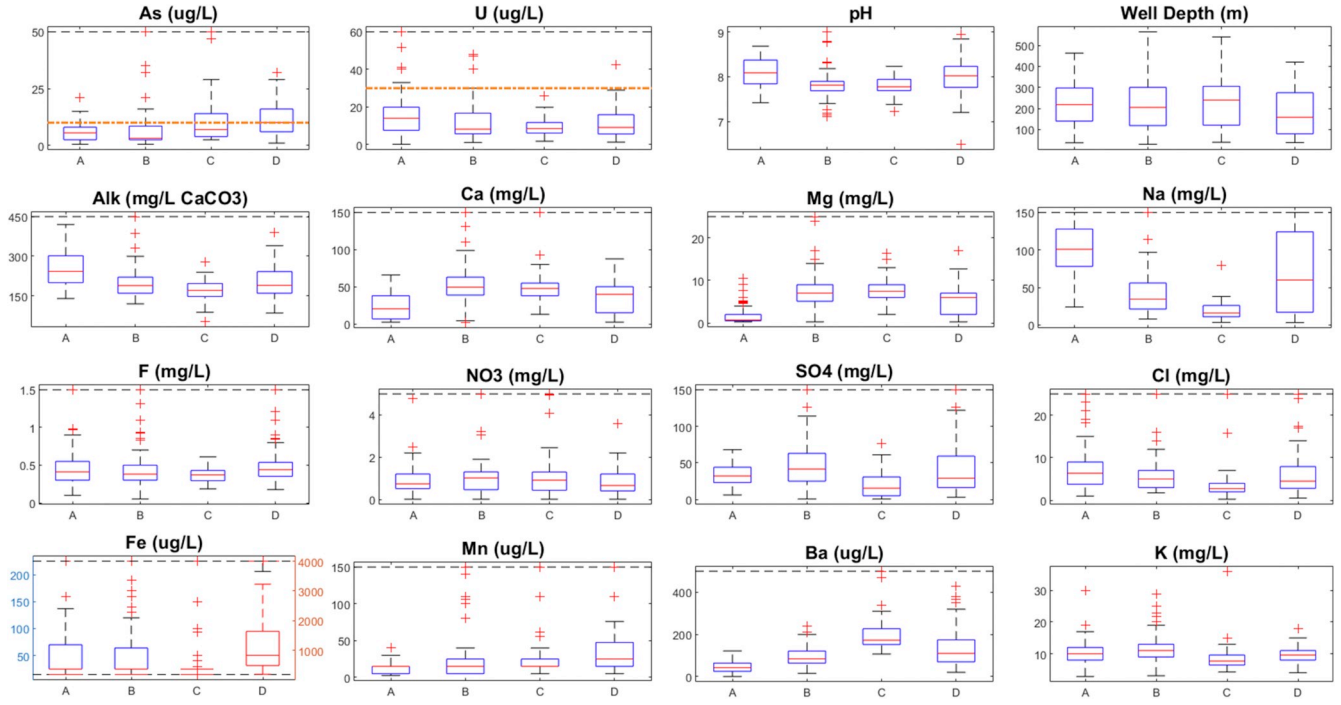

Fig. 6. Boxplots showing distributions of the various hydrogeochemical parameters for the 4 geochemical regions A-D. MCLs are highlighted for As and U using a dashed orange line. The dashed black line indicates the presence outliers greater than the scale shown in the y-axis. Note separate y-axis scales in the iron boxplot: Regions A, B, and D are plotted on the left (blue) scale and Region C is plotted on the right (red) scale. (For interpretation of the references to color in this figure legend, the reader is referred to the Web version of this article.)

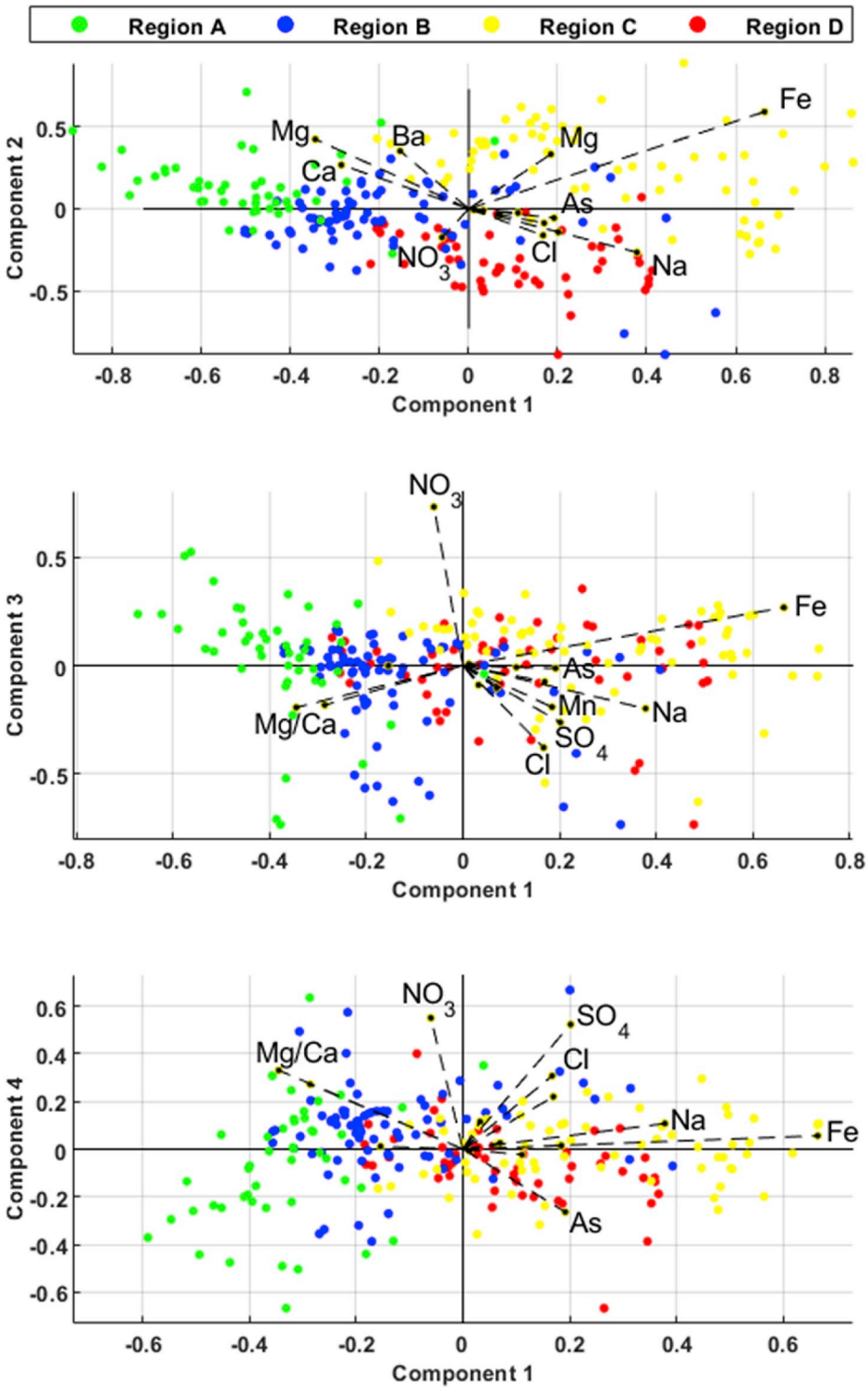

Fig. 7. Biplots of the four principal components, showing separation of geochemical regions and relative importance of geochemical parameters on delineating geochemical regions (the magnitude of the vector indicates its relative importance on each of the principal components). PCA-transformed data for each wellbore sample are plotted as dots and vectors for each of the geochemical parameters are plotted as dashed lines.

aquifer.

4.4. Geochemical equilibrium modeling

Equilibrium modeling was used to assess how mineral precipitation and dissolution in the four major geochemical environments may alter metal mobility within the Arikaree aquifer. Mineral saturation index (SI) was calculated in GWB using composite geochemistry for each major group/region (Table 4).

Calcite saturation increases along the Arikaree aquifer flowpaths from Region A to Region D, indicating that calcite precipitation likely occurs. Fe concentrations are higher in Regions C and D, leading to higher calculated SIs for iron containing phases. Without measurements of redox conditions, which were not collected for this collated dataset, it

Table 4
Saturation indices (SI) of minerals across the four geochemical regions of the PRR. If SI is > 0 minerals will tend to precipitate, if SI < 0 minerals will dissolve if present in the rocks, and dashed lines (–) indicates that the SI was sufficiently small to not be considered (in this case, SI < −3.0).

Mineral	Region A	Region B	Region C	Region D
Calcite	0.51	0.59	0.65	0.61
Siderite	−0.86	−0.68	1.1	−0.24
Dolomite	−0.21	−0.025	0.034	−0.25
Barite	0.10	0.24	0.38	−0.33
Gypsum	−2.5	−1.9	−2.4	−2.6
$Fe(OH)_3$	–	–	−1.5	−2.9

is difficult to quantitively interpret how reactions involving iron phases (e.g. $Fe(OH)_3$) might be controlling As and U behavior. However, the presence of higher Fe concentrations in Regions C and D and calculated SIs suggest that formation of iron precipitates may occur in downgradient sections of the Arikaree aquifer, which may in turn act as sorption surfaces for As and U.

Geochemical modeling may be useful to parse potential transformation pathways. Fe (hydr)oxides are minimally soluble, but may act as a sorption surface for As and U, limiting their subsurface mobility. In downgradient portions of the Arikaree aquifer, such as Regions C and D, groundwater has higher alkalinity and pH, which may decrease sorption affinity of As and U while simultaneously making complexation with ligands more favorable, enhancing As and U mobility via formation of stable aqueous complexes. Complexation reactions and sorption/desorption kinetics may be an important factor for As and U mobility in downgradient portions of the Arikaree aquifer.

5. Discussion

The statistical, spatial and geochemical analyses indicate that there are four hydrogeochemical environments within the Arikaree aquifer, which reflect evolution of groundwater geochemistry. Differences between these four geochemical regions are detailed here.

5.1. Region A (n of wells = 46)

Region A had the lowest pH, mineral SIs, alkalinity, and Na^+ levels and was spatially clustered in the upgradient, southern portion of the Arikaree aquifer, or proximal to contacts between the upper extent of the Arikaree and overlying sediments. Wells in this region had an average depth of 64.6 m. PCA and Piper diagram analysis show groundwater samples from Region A are enriched in Ca^{2+} and Mg^{2+} (Fig. 7). This upgradient, recharge-dominated portion of the Arikaree aquifer had the lowest levels of As and U, suggesting that recharge processes may limit As and U mobility in this portion of the aquifer due to input of low pH, low alkalinity water, as well as limited water-rock contact time.

5.2. Region B (n of wells = 80)

Wells in Region B are generally drilled to a similar depth as in Region A (mean depth = 63.4 m), and were located in the southern or central portions of the Arikaree aquifer. Groundwaters sampled from these wells are characterized by low pH and moderate alkalinity. Mineral saturation is typically higher compared to Region A, and dolomite saturation increases to near equilibrium levels in Region B, indicating that precipitation of a mixed Mg^{2+} - Ca^{2+} carbonate phase may begin to appear in this intermediate portion of the Arikaree aquifer. PCA shows that Region B is similar to Region A but has slightly higher Na^+ and Fe^{2+} levels. As and U levels remain relatively low in Region B, and this region likely represents a transition from the upgradient portion of the aquifer where influences from recharge decrease and mineral dissolution becomes a stronger influence on solute concentrations as water-rock contact time increases.

5.3. Region C (n of wells = 67)

Wells in Region C are generally slightly deeper than Regions A and B (mean depth = 66.4 m) and drilled into the central to northern portions of the Arikaree aquifer. Na^+ and pH levels rise in this region of the aquifer, while alkalinity remains moderate. Fe levels in Region C are over an order of magnitude greater than any of the other geochemical regions (Fig. 6), and siderite ($FeCO_3$) saturation indices are positive, indicating possible precipitation of an $FeCO_3$ phase. Calcite and dolomite saturation increase compared to Region B suggesting that carbonate precipitation becomes more favorable, which could act as a sink for aqueous carbonate species. PCA suggests that Fe and Mn are the distinguishing factors for Region C, as well as Na^+ and As to a lesser extent. Both As and U concentrations increase in this region of the Arikaree aquifer, and average As concentrations are above the MCL (~12 μg/L). Dissolution of Fe (hydr)oxides and release of adsorbed metals may enhance As and U mobility in this region.

This region has the greatest mean well depth, and may screen wells in the basal portion on the Arikaree aquifer which is enriched in Fe hydr (oxides) and volcanic ash. The spatial extent of subfacies within the Arikaree aquifer such as the Sharps Formation and Rockyford Ash Zone (Table 1) are poorly characterized on the PRR, but could explain the major discrepancy in Fe concentrations in this region.

5.4. Region D (n of wells = 54)

Wellbores in Region D have the highest pH, alkalinity, and Na^+ levels as well as the highest As and U concentrations. Wellbores in this region likely represent a downgradient endmember within the Arikaree aquifer, where mature groundwater has become enriched in carbonate alkalinity and Na^+ due to mineral dissolution, ion exchange, and/or leaching of volcanic ash along flowpaths of the aquifer which drives up pH. This region is generally clustered in the northern, farthest downgradient section of the Arikaree aquifer and had the shallowest mean well depth (54.7 m) of all the hydrogeochemical groupings. PCA analysis shows that Na^+ has the strongest loading on Region D (Fig. 7). Carbonate SI's remain supersaturated in this region, suggesting that precipitation of carbonate minerals may influence groundwater chemistry, acting as a carbonate sink and reducing carbonate alkalinity. However, this downgradient portion of the Arikaree aquifer is proximal to volcanic ash deposits in the basal Arikaree and White River Group (Sibray, 2011), which are a known geogenic metal source in southwestern South Dakota, and volcanic ash in this basal portion of the aquifer may act as a secondary source of alkalinity. Groundwater quality on the PRR may be heavily influenced by ash deposits, given that ash may act as a source for both metals and metal mobilizing alkalinity. As groundwater flows downgradient in the Arikaree aquifer, pH and alkalinity increase, with Na^+ replacing Ca^{+2} as the dominant cation, which limits sorption affinity and enhances As and U mobility on the PRR. Similar controls of As and U mobility have been noted in other studies (e.g. Ayotte et al., 2011; Riedel and Kübeck, 2018; Scanlon et al., 2009), indicating that groundwater residence time and formation water maturity in the Arikaree aquifer may be key controls of As and U mobility on the PRR.

6. Conclusions

Here, we explored underlying controls to As and U mobility in 253 groundwater chemistry samples from the PRR using various statistical and geochemical methods. Our conceptual model indicates that water quality degrades along the flow direction of the Arikaree aquifer. The southern, upgradient sections of the Arikaree aquifer are influenced by recharge of meteoric water that keeps groundwater pH and alkalinity relatively low, which limits As and U mobility. As groundwater flows

through the Arikaree aquifer, pH and alkalinity rise due to mineral dissolution and, potentially, leaching of volcanic ash from the basal portion of the Arikaree aquifer, which increases As and U mobility. Human health impacts from high As and U levels are more likely in the downgradient sections of the Arikaree aquifer, such as the northern extent of the PRR. The dataset obtained from IHS indicated that 32% of wells exceeded the MCL for arsenic, 8% exceeded the uranium MCL, and 23% exceeded the MCL for gross alpha, highlighting the critical need for continued investigation as thousands of people on the PRR rely on the Arikaree aquifer as their drinking water source.

Funding source

This work was supported by the Bill & Melinda Gates Foundation, Seattle, WA.

Declaration of competing interest

The authors have no conflicts of interest to declare.

Acknowledgements

This work would not have been possible without collaboration with the Oglala Sioux Tribe and the Indian Health Service Office of Martin, South Dakota. We would also like to thank Dr. Richard Wanty for lending his expertise in radionuclide geochemistry.

Appendix A. Supplementary data

Supplementary data to this article can be found online at https://doi.org/10.1016/j.apgeochem.2020.104522.

References

Abdi, H., Williams, L.J., 2010. Principal component analysis. Wiley Interdiscip. Rev.: Comput. Stat. 2 (4), 433–459. https://doi.org/10.1002/wics.101.

Adler, H.H., 1963. Concepts of genesis of sandstone-type uranium ore deposits. Econ. Geol. 58, 839–852. https://doi.org/10.2113/gsecongeo.58.6.839.

Archuleta, C.-A.M., Constance, E.W., Arundel, S.T., Lowe, A.J., Mantey, K.S., Phillips, L. A., 2017. The National Map seamless digital elevation model specifications. U. S. Geol. Surv. Methods 11-B9, 39. https://doi.org/10.3133/tm11B9.

Armienta, M.A., De la Cruz-Reyna, S., Cruz, O., Ceniceros, N., Aguayo, A., Marin, M., 2011. Fluoride in ash leachates: environmental implications at Popocatépetl volcano, central Mexico. Nat. Hazards Earth Syst. Sci. 11 (7), 1949–1956. https://doi.org/10.5194/nhess-11-1949-2011.

Ayotte, J.D., Szabo, Z., Focazio, M.J., Eberts, S.M., 2011. Effects of human-induced alteration of groundwater flow on concentrations of naturally-occurring trace elements at water-supply wells. Appl. Geochem. 26 (5), 747–762. https://doi.org/10.1016/j.apgeochem.2011.01.033.

Beaucaire, C., Toulhoat, P., 1987. Redox chemistry of uranium and iron, radium geochemistry, and uranium isotopes in the groundwaters of the Lode've Basin, Massif Central, France. Appl. Geochem. 2, 417–426. https://doi.org/10.1016/0883-2927(87)90025-4.

Blake, J.M., De Vore, C.L., Avasarala, S., Ali, A.-M., Roldan, C., Bowers, F., Spilde, M.N., Artyushkova, K., Kirk, M.F., Peterson, E., Rodriguez-Freire, L., Cerrato, J.M., 2017. Uranium mobility and accumulation along the rio paguate, jackpile mine in laguna pueblo, NM. Environ. Sci. Process. Impacts 19, 605–621. https://doi.org/10.1039/C6EM00612D.

Bowell, R.J., 1994. Sorption of arsenic by iron oxides and oxyhydroxides in soils. Appl. Geochem. 9, 279–286. https://doi.org/10.1016/0883-2927(94)90038-8.

Bowell, R.J., Alpers, C.N., Jamieson, H.E., Nordstrom, D.K., Majzlan, J., 2014. The environmental geochemistry of arsenic – an overview –. Rev. Mineral. Geochem. 79, 1–16. https://doi.org/10.2138/rmg.2014.79.1.

Bozdogan, H., 1987. Model selection and Akaike's Information Criterion (AIC): the general theory and its analytical extensions. Psychometrika 52 (3), 345–370. https://doi.org/10.1007/BF02294361.

Braithwaite, A., Livens, F.R., Richardson, S., Howe, M.T., Goulding, K.W.T., 2008. Kinetically controlled release of uranium from soils. Eur. J. Soil Sci. 48, 661–673. https://doi.org/10.1111/j.1365-2389.1997.tb00566.x.

Carter, J.M., Heakin, A.J., 2007. Generalized Potentiometric Surface of the Arikaree Aquifer, Pine Ridge Indian Reservation and Bennett County, South Dakota: U.S. Geological Survey Scientific Investigations Map 2993, 2 sheets.

Carter, J.M., Sando, S.K., Hayes, T.S., Survey, Hammond, R.H., 1997. Source, Occurrence, and Extent of Arsenic in the Grass Mountain Area of the Rosebud Indian Reservation, South Dakota. USGS Water Resources Investigation Report, pp. 97–4286.

Colman, J.A., 2011. Arsenic and Uranium in Water from Private Wells Completed in Bedrock of East-Central Massachusetts— Concentrations, Correlations with Bedrock Units, and Estimated Probability Maps. USGS Scientific Investigations. Report 2011-5013.

Cumberland, S.A., Douglas, G., Grice, K., Moreau, J.W., 2016. Uranium mobility in organic matter-rich sediments: a review of geological and geochemical processes. Earth Sci. Rev. https://doi.org/10.1016/j.earscirev.2016.05.010. Elsevier B.V.

Davis, J.C., 2002. Statistics and Data Analysis in Geology. J. Wiley.

Dickinson, K.A., 1993. Favorable Areas for Uranium in the Oligocene White River Beds of Southwestern South Dakota, Southeastern Wyoming and Northwestern Nebraska. USGS Open File Rep, pp. 93–624.

Focazio, M.J., Welch, A.H., Watkins, S.A., Helsel, D.R., Horn, M.A., 1999. A Retrospective Analysis on the Occurrence of Arsenic in Ground-Water Resources of the United States and Limitations in Drinking-Water-Supply Characterizations. USGS Water Resource Investigation Report, pp. 99–4279.

Gjelsteen, T.W., Collings, S.R., 1988. Relationship between groundwater flow and uranium mineralization IN the chadron formation, northwest Nebraska. East. In: Powder River Basin - Black Hills 39th Annual Field Conference Guidebook, pp. 271–284.

Hansley, B.P., Collings, S., Brownfield, K., Skipp, G., 1989. Mineralogy of Uranium Ore from the Crow Butte Uranium Deposit, Oligocene Chadron Formation, Northwestern Nebraska, vol. 225. USGS Open-File Rep.

Heakin, A.J., 2000. Water Quality of Selected Springs and Public-Supply Wells, Pine Ridge Indian Reservation, South Dakota, 1992-97. USGS Water-Resources Investig. Report 99-4063.

Helsel, D.R., Hirsch, R.M., 2002. Statistical methods in water resources. In: Techniques of Water-Resources Investigations Book 4, Hydrologic Analysis and Interpretation. U.S. Geological Survey.

Hirsch, R.M., Alexander, R.B., Smith, R.A., 1991. Selection of methods for the detection and estimation of trends in water quality. Water Resour. Res. 27 (5), 803–813. https://doi.org/10.1029/91WR00259.

Holm, T.R., 2002. Effects of CO 3 2-/bicarbonate, Si, and PO 4 3- on Arsenic sorption to HFO. Am. Water Works Assoc. 94 (4), 174–181. https://doi.org/10.1002/j.1551-8833.2002.tb09461.x.

U.S. EPA, IHS, U.D., 2008. Meeting the access goal: strategies for increasing access to safe drinking water and wastewater treatment to American Indian and Alaska native villages. https://www.epa.gov/tribal/meeting-access-goal-strategies-increasing-access-safe-drinking-water-and-wastewater-treatment.

Indian Health Service, 2018. Indian health disparities fact sheets. https://www.ihs.gov/newsroom/includes/themes/responsive2017/display_objects/documents/factsheets/Disparities.pdf.

Jolliffe, I.T., 2002. Principal Component Analysis, second ed. Springer, New York. https://doi.org/10.1007/B98835.

Jones, D.S., 2006. The persistence of American Indian health disparities. Am. J. Public Health 96, 2122–2134. https://doi.org/10.2105/AJPH.2004.054262.

Kipp, G.G., Stone, J.J., Stetler, L.D., 2009. Arsenic and uranium transport in sediments near abandoned uranium mines in Harding County, South Dakota. Appl. Geochem. 24, 2246–2255. https://doi.org/10.1016/J.APGEOCHEM.2009.09.017.

LaGarry, H., Yellow Thunder, E., 2012. Surface and subsurface distribution of uranium-bearing strata in NW Nebraska and SW South Dakota. In: Nebraska Academy of Science.

Lee, J.S., Nriagu, J.O., 2002. Arsenic carbonate complexes in aqueous systems. In: Biogeochemistry of Environmentally Important Trace Metals, pp. 33–41. https://doi.org/10.1021/bk-2003-0835.ch003.

Lewis, J., Hoover, J., MacKenzie, D., 2017. Mining and environmental health disparities in native American communities. Curr. Environ. Health Rep. 4, 130–141. https://doi.org/10.1007/s40572-017-0140-5.

Martin, J.E., Sawyer, J.F., Fahrenbach, M.D., Tomhave, D.W., Schulz, L.D., 2004. Geologic map of south Dakota. South Dakota dep. Environ. Nat. Resour. Gen. Map 10.

Masuda, H., 2018. Arsenic cycling in the Earth's crust and hydrosphere: interaction between naturally occurring arsenic and human activities. Prog. Earth Planet. Sci. 5 (1), 68. https://doi.org/10.1186/s40645-018-0224-3.

McConnell, T.H., Dibenedetto, J.N., 2012. Geology of the early arikareean Sharps Formation on the Pine Ridge Indian reservation and surrounding areas of south Dakota and Nebraska. PLoS One 7, e47759. https://doi.org/10.1371/journal.pone.0047759.

Meng, S.X., Maynard, J.B., 2001. Use of statistical analysis to formulate conceptual models of geochemical behavior: water chemical data from the Botucatu aquifer in São Paulo state, Brazil. J. Hydrol. 250, 78–97. https://doi.org/10.1016/S0022-1694(01)00423-1.

Milvy, P., Cothern, R., 1990. Scientific background for the development of regulations for radionuclides in drinking water. In: Radon, Radium, and Uranium in Drinking Water. Lewis Publishers, Chelsea, MI, pp. 1–16.

Nagorski, S.A., Moore, J.N., 1999. Arsenic mobilization in the hyporheic zone of a contaminated stream. Water Resour. Res. 35, 3441–3450. https://doi.org/10.1029/1999WR900204.

Nolan, J., Weber, K.A., 2015. Natural uranium contamination in major U.S. Aquifers linked to nitrate. Environ. Sci. Technol. Lett. 2, 215–220. https://doi.org/10.1021/acs.estlett.5b00174.

Nordstrom, D.K., Majzlan, J., Konigsberger, E., 2014. Thermodynamic properties for arsenic minerals and aqueous species. Rev. Mineral. Geochem. 79, 217–255. https://doi.org/10.2138/rmg.2014.79.4.

Pang, Y., Peng, R.D., Jones, M.R., Francesconi, K.A., Goessler, W., Howard, B.V., Umans, J.G., Best, L.G., Guallar, E., Post, W.S., Kaufman, J.D., Vaidya, D., Navas-Acien, A., 2016. Metal mixtures in urban and rural populations in the US: the multi-

ethnic study of atherosclerosis and the strong heart study. Environ. Res. 147, 356–364. https://doi.org/10.1016/j.envres.2016.02.032.
Rahn, P.H., Paul, H.A., 1975. Hydrogeology of a portion of the sand Hills and ogallala aquifer, south Dakota and Nebraska. Gr. Water 13, 428–437. https://doi.org/10.1111/j.1745-6584.1975.tb03610.x.
Raymond, W.H., Gries, J.P., King, R.U., 1976. Status of mineral resource information for the pine ridge indian reservation, South Dakota, vol. 12. USGS Administrative Report BIA –.
Riedel, T., Kübeck, C., 2018. Uranium in groundwater – a synopsis based on a large hydrogeochemical data set. Water Res. 129, 29–38. https://doi.org/10.1016/j.watres.2017.11.001.
Rogers, D., Petereit, D., 2005. Cancer disparities research partnership in Lakota county: clinical trials, patient services, and community education for the Oglala, rosebud, and Cheyenne river Sioux tribes. Am. J. Public Health 95.
Scanlon, B.R., Nicot, J.P., Reedy, R.C., Kurtzman, D., Mukherjee, A., Nordstrom, D.K., 2009. Elevated naturally occurring arsenic in a semiarid oxidizing system, Southern High Plains aquifer, Texas, USA. Appl. Geochem. 24 (11), 2061–2071. https://doi.org/10.1016/j.apgeochem.2009.08.004.
Shacklette, H.T., Boerngen, J.G., 1984. Element Concentrations in Soils and Other Surficial Materials of the Conterminous United States. USGS Prof. Pap, p. 1270.
Sibray, S., 2011. Potential uranium source rocks of the White River group in western Nebraska and south Dakota. AAPG search and discovery. Article #80186. http://www.searchanddiscovery.com/documents/2011/80186sibray/ndx_sibray.pdf.
Singh, A., 2010. Geochemical conditions affecting uranium(VI) fate and transport in soil and groundwater in the presence of phosphate. All Theses and Dissertations 324. http://openscholarship.wustl.edu/etd/324.
Smith, A.H., Hopenhayn-Rich, C., Bates, M.N., Goeden, H.M., Hertz-Picciotto, I., Duggan, H.M., Wood, R., Kosnett, M.J., Smith, M.T., 1992. Cancer risks from arsenic in drinking water. Environ. Health Perspect. 97, 259–267.
Stollenwerk, K.G., 2005. Geochemical processes controlling transport of arsenic. Groundwater: a review of adsorption. In: Arsenic in Ground Water. Kluwer Academic Publishers, pp. 67–100. https://doi.org/10.1007/0-306-47956-7_3.
U.S. Census Bureau, 2010. 2010 Demographic Profile Data. DP-1.
U.S. EPA, 1991a. Manual of Individual and Non-Public Water Supply Systems. https://nepis.epa.gov/Exe/ZyPURL.cgi?Dockey=2000U9HN.TXT.
U.S. EPA, 1991b. Regional Guidance on Handling Chemical Concentration Data Near the Detection Limit in Risk Assessments. Regional Technical Guidance Manual, Risk Assessment. https://www.epa.gov/risk/regional-guidance-handling-chemical-concentration-data-near-detection-limit-risk-assessments.
U.S. EPA, 2000. National primary drinking water regulations; radionuclides; final rule. Fed. Regist. 65, 76707–76753.
U.S. EPA, 2001. Technical Fact Sheet: Final Rule for Arsenic in Drinking Water. https://nepis.epa.gov/Exe/ZyPURL.cgi?Dockey=20001XXE.TXT.
U.S. EPA, 2015. Regulation Timeline: Contaminants Regulated Under the Safe Drinking Water Act. https://www.epa.gov/dwregdev/regulation-timeline-contaminants-regulated-under-safe-drinking-water-act.
van Berk, W., Fu, Y., 2017. Redox roll-front mobilization of geogenic uranium by nitrate input into aquifers: risks for groundwater resources. Environ. Sci. Technol. 51, 337–345. https://doi.org/10.1021/acs.est.6b01569.
Waite, T.D., Davis, J.A., Payne, T.E., Waychunas, G.A., Xu, N., 1994. Uranium(VI) adsorption to ferrihydrite: application of a surface complexation model. Geochem. Cosmochim. Acta 58 (24), 5465–5478. https://doi.org/10.1016/0016-7037(94)90243-7.
Wold, S., Esbensen, K., Geladi, P., 1987. Principal component analysis. Chemometr. Intell. Lab. Syst. 2 (1–3), 37–52. https://doi.org/10.1016/0169-7439(87)80084-9.
Zachara, J.M., Long, P.E., Bargar, J., Davis, J.A., Fox, P., Fredrickson, J.K., Freshley, M. D., Konopka, A.E., Liu, C., McKinley, J.P., Rockhold, M.L., Williams, K.H., Yabusaki, S.B., 2013. Persistence of uranium groundwater plumes: contrasting mechanisms at two DOE sites in the groundwater–river interaction zone. J. Contam. Hydrol. 147, 45–72. https://doi.org/10.1016/J.JCONHYD.2013.02.001.